JOURNAL OF GEOPHYSICAL RESEARCH, VOL. 112, D15103, doi:10.1029/2007JD008510, 2007

Doubled length of western European summer heat waves since 1880

P. M. Della-Marta,[1,2,3] M. R. Haylock,[4] J. Luterbacher,[1,5] and H. Wanner[1,5]

Received 5 February 2007; revised 27 April 2007; accepted 16 May 2007; published 3 August 2007.

[1] We analyzed a new data set of 54 high-quality homogenized daily maximum temperature series from western Europe (Austria, Belgium, Croatia, Czech Republic, Denmark, Finland, France, Germany, Ireland, Netherlands, Portugal, Spain, Sweden, Switzerland, United Kingdom) to define more accurately the change in extreme warm Daily Summer Maximum Temperature (DSMT). Results from the daily temperature homogeneity analysis suggest that many instrumental measurements in the late 19th and early 20th centuries were warm-biased. Correcting for these biases, over the period 1880 to 2005 the length of summer heat waves over western Europe has doubled and the frequency of hot days has almost tripled. The DSMT Probability Density Function (PDF) shows significant changes in the mean (+1.6 ± 0.4°C) and variance (+6 ± 2%). These conclusions help further the evidence that western Europe's climate has become more extreme than previously thought and that the hypothesized increase in variance of future summer temperature has indeed been a reality over the last 126 years.

Citation: Della-Marta, P. M., M. R. Haylock, J. Luterbacher, and H. Wanner (2007), Doubled length of western European summer heat waves since 1880, *J. Geophys. Res.*, *112*, D15103, doi:10.1029/2007JD008510.

1. Introduction

[2] Extreme temperature events such as the 2003 European heat wave have an unprecedented impact on our society and economy [*Kovats and Koppe*, 2005; *Poumadere et al.*, 2005]. In order to help predict the occurrence of these events, it is important to have a reliable set of observations [*Intergovernmental Panel on Climate Change* (*IPCC*), 2001], as a basis to investigate the physical mechanisms responsible for their evolution [*Kiktev et al.*, 2003; *Meehl and Tebaldi*, 2004; *Schär et al.*, 2004; *Stott et al.*, 2004; *Brabson et al.*, 2005; *Cassou et al.*, 2005; *Christidis et al.*, 2005; *Findell and Delworth*, 2005; *Ferranti and Viterbo*, 2006; *Sutton and Hodson*, 2005; *Seneviratne et al.*, 2006; *Vautard et al.*, 2007; *Della-Marta et al.*, 2007] and to develop ways to improve our adaptation to these events, especially for those most vulnerable to them [*Kovats and Koppe*, 2005]. With the observed and projected increase in the frequency of extreme warm temperatures, many places in the world will face an increasing risk of such events [*IPCC*, 2001; *Alexander et al.*, 2006].

[3] Numerous studies have applied extreme value theory to the topic of temperature change [*Mearns et al.*, 1984; *Katz and Brown*, 1992; *Schär et al.*, 2004]. These studies conclude that a change in variance of the temperature Probability Density Function (PDF) has a greater impact on the frequency and duration of extremes than just a shift in the mean. Recent studies show that by 2071, summer temperature variability is expected to have increased by up to 100% in central Europe [*Schär et al.*, 2004; *Weisheimer and Palmer*, 2005]. Furthermore, studies have shown a significant increase in the variance of daily temperature since 1976 [*Klein Tank and Können*, 2003; *Klein Tank et al.*, 2005]. However, because published studies only utilize short data sets, there is little evidence to suggest that this recent trend in temperature variance differs from some longer-term cyclic variation of the climate system. This study aims to answer this question using a high-quality daily maximum temperature data set which has been homogenized at the daily timescale. We quantify the effect of changes in the Daily Summer Maximum Temperature (DSMT) PDF on two extreme indices and show evidence that early daily temperature records are generally warm-biased and that current estimates of changes in June-August extreme daily temperatures [e.g., *Klein Tank and Können*, 2003; *Alexander et al.*, 2006; *Moberg et al.*, 2006] have hitherto been conservative in their estimate of changes in extremes over the last 126 years. We also discuss the spatial variability of observed changes in the DSMT PDF over western Europe and compare them to expected future changes.

2. Data and Methods

2.1. DSMT Data and Their Homogenization

[4] The 54 daily maximum temperature records were checked for basic quality, including logic tests with other elements (e.g., maximum temperature greater than the minimum temperature, etc.) and obviously erroneous outliers which were removed [*Moberg et al.*, 2006]. Where possible, we used station series which had been homoge-

[1]Institute of Geography, University of Bern, Bern, Switzerland.
[2]Federal Office for Meteorology and Climatology, MeteoSwiss, Zurich, Switzerland.
[3]Bureau of Meteorology, National Climate Centre, Melbourne, Australia.
[4]Climatic Research Unit, University of East Anglia, Norwich, UK.
[5]National Center of Competence in Research on Climate (NCCR), Bern, Switzerland.

0148-0227/07/2007JD008510$09.00

nized at the daily timescale by other studies (a total of 44 stations), 25 of these stations were homogenized using a new method [*Della-Marta and Wanner*, 2006] that is capable of correcting the mean and also the higher order moments of inhomogeneities typically found in instrumental series [*Della-Marta et al.*, 2007]. During the homogenization procedure, steps were taken to try and minimize the influence of urban warming; however, it is probable that some time series are not totally free from this phenomenon. See our recent work [*Della-Marta et al.*, 2007] for detailed station information and the homogeneity procedure applied to each. A total of 44 homogenized daily maximum temperature records were used, whereas only 10 entered the data set which could not be homogenized due to limitations in the amount of metadata available to our recent work [*Della-Marta et al.*, 2007] and to that of *Moberg et al.* [2006]. However, these stations were carefully scrutinized for consistency, obvious inhomogeneities, and outliers before entering the data set. Not all 54 station records start in 1880. See our recent work [*Della-Marta et al.*, 2007] for details on the starting dates of each record. Around half of the stations (28) had data in 1880, with the number of stations reaching the maximum number 54 by 1906.

2.2. The Hot Day and Heat Wave Indices

[5] A hot day is defined as a day where the daily maximum temperature exceeds the long-term daily 95th percentile of daily maximum temperature. The hot day index (HD) is the number of such days within a June-August season expressed as a percentage of time. A heat wave (HW) is defined as the maximum number of consecutive days where the DSMT exceeds the long-term daily 95th percentile of DSMT within a June-August season. For each day of the 92 days in the June-August period, a 95th percentile is calculated from a sample of 15 days (7 days either side of the day) using data over the 1906 to 1990 period. This gives a sample of 1275 days (the number of observations in each box of Figure 1) from which a 95th percentile is calculated empirically (Figure 1, black line). Figure 1 shows the daily 95th percentile for Paris. The 95th percentile shows seasonal variation of approximately 4°C, with generally lower thresholds in the beginning and end of summer and a peak around day 38 of the summer season. The seasonal variation of the daily 95th percentile, shown in Figure 1, is typical of many stations in the data set. For comparison purposes, the 95th percentile calculated for the entire season is shown (Figure 1, thick black dashed line). As expected, this percentile calculation falls between the daily 95th percentiles.

[6] Figure 2 shows diagrammatically how the HD and HW index are calculated using Paris daily data from summer 2003. The bold black open circles indicate HDs and the grey box shows the maximum length HW. If a seasonal percentile is used (Figure 2, black dashed line), then the number of HDs is likely to be underestimated in the beginning of the summer season since the seasonal percentile is higher than the daily percentiles at this time in the season (Figure 2, black line). For this reason, we chose to use daily percentiles in order to account for seasonal variation.

2.3. Trend Analysis

[7] In order to reduce the effects of extreme seasons in our data set overly affecting the estimation of a long-term trend (especially at the beginning and the end of a time series), we used a robust method of fitting of linear models (Robust Linear Model, RLM) called *M*-estimators [*Venables and Riply*, 2002], a technique which replaces the minimization of the squared residuals (as in ordinary least squares) by the minimization of some other function less sensitive to outliers. Here we used a Huber function [*Venables and Riply*, 2002].

[8] To determine the statistical significance of trends, we used either the standard error of the RLM slope parameter or Kendall's Tau, a nonparametric statistic suitable for detecting the significance of trends in data sampled from nonnormal distributions. All trend confidence intervals assume a *t*-distributed estimate of standard error of the RLM slope parameter. However, since in all cases the degrees of freedom of the RLM fits are above 60, the standard error of the estimated slope was multiplied by 1.96 to give an approximate 95% confidence interval.

[9] In the assessment of the relationship between the mean and the variance, we used a linear model fitted using Total Least Squares (TLS), a method which is more suitable than Ordinary Least Squares (OLS) when both the regression variates have errors associated which their measurement [*De Groen*, 1996].

2.4. Filtering of Time Series

[10] The decadal filtering of time series was performed using a local regression smoother [*Venables and Riply*, 2002]. The smoothing parameter was set at a cut-off of approximately 10 years.

2.5. Assessment of Probability Density Function (PDF) Changes

[11] We assessed changes in the PDF of DSMT and the extreme indices (HD and HW) by fitting a Generalized Extreme Value (GEV) distribution and a Gamma distribution to the data, respectively, using the theory of *L*-Moments [*Hosking*, 1990]. This method determines statistical moments of a sample that are more robust estimates of the underlying distribution in the presence of outliers and/or small samples than conventional moment calculations [*Hosking*, 1990]. The DSMT data from each station were standardized by the long-term mean and standard deviation (1906 to 1990 period) and were split into 9 (4) independent periods to assess the changes in the DSMT (extreme indices). In order to separate intrinsic variance changes from long-term trend-induced variance changes, the data in each independent period were piecewise detrended [*Scherrer et al.*, 2005]. We define intrinsic variance as the variance remaining in the time series once decadal and longer timescale variability has been removed. All conclusions drawn from the PDF change calculations are robust to the exclusion of the year 2003. A more detailed description of this method is given below.

[12] The DSMT data at station s is given by $X_s = \{x_s(i) : i = 1, \ldots, N_s\}$, where N_s equals the number of daily maximum temperature measurements in the June-August season, 92 multiplied by the number of years in the record give $N_s \leq 11{,}592$ where $s \in \{1, \ldots, n_s\}$ and $n_s = 54$. Firstly, in order to be able to compare the PDFs of all stations across the domain, the observations were standardized by the long-term mean (μ_s) and standard deviation (σ_s) calculated over 1906 to 1990 (we chose this period since we believe

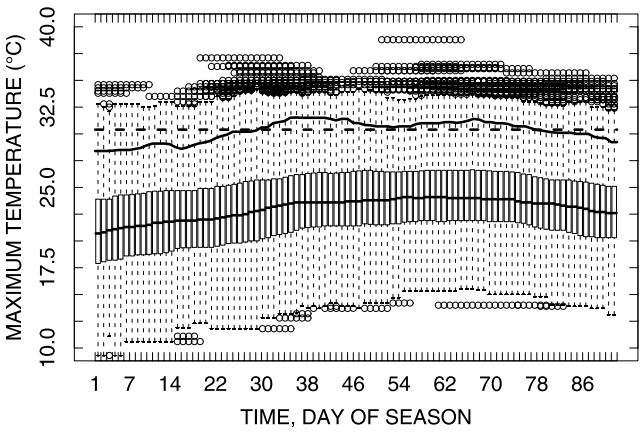

Figure 1. The daily DSMT 95th percentile for Paris (black line), calculated using data from 1906 to 1990. The thick dashed black line is the seasonal 95th percentile (based on all seasonal data). Each box plot represents the distribution of the daily data used to calculate each daily empirical 95th percentile. The box plots show the median (solid black line in the middle of the box), interquartile range (boundaries of the box), and 1.5 times the interquartile range (outer lines) and observations outside this range (open circles).

that it is more representative of the average 20th century climate than the 1961 to 1990 period) following *Katz and Brown* [1992] according to equation (1).

$$Z_s = \frac{X_s - \mu_s}{\sigma_s} \tag{1}$$

For each daily station record in each of the 9 independent periods, k (14 years in length, 1880 to 1893, 1894 to 1905, …, 1992 to 2005), the daily data were split according to equation (2).

$$Z_{s,k} = \{z_s(i) : i = \rho(k), \rho(k)+1, \ldots, \rho(k)+N_{s,k}-1\} \tag{2}$$

Where $\rho(k) = (k-1)N_{s,k} + 1$, $k = \{1, \ldots, 9\}$ and $N_{s,k} = 14 \times 92 = 1288$. The $Z_{s,k}$ for each s and k were detrended according to equation (3) in order to remove any artificial change in the variance due to decadal variability [*Scherrer et al.*, 2005], where $\alpha_{s,k}$ and $\beta_{s,k}$ are the intercept and slope terms, respectively, of an Ordinary Least Squares (OLS) model for each period k. The mean of each period, $\bar{Z}_{s,k}$, was added back to the data in this period k to allow the differences in mean of each PDF to be seen.

$$z^*_{s,k}(i) = z_{s,k}(i) - \left(\alpha_{s,k} + \beta_{s,k} \cdot x_s(i)\right) + \bar{Z}_{s,k}\Big) \tag{3}$$

Where $i = \{1, \ldots, N_{s,k}\}$, $k = \{1, \ldots, 9\}$, and $\bar{Z}_{s,k} = \frac{1}{N_{s,k}} \sum_{i=1}^{N_{s,k}} = z_{s,k}(i)$. Figure 3 is a conceptual diagram [*Scherrer et al.*, 2005] that demonstrates the effect of equation (3). Figure 3a shows a series with constant variance over time but with a perfectly linear trend and the corresponding PDFs for each of the 3 independent periods is shown in Figure 3b. In this case, the variance of the PDFs is artificially inflated due to the linear trend. If the intrinsic variance remains constant but the overall trend is quadratic (Figure 3c), then the effect of the quadratic trend on the shape of the PDFs (Figure 3d) is more clearly shown. Figure 3f demonstrates that when we apply equation (2) to the series shown in Figure 3c, we see no change in the shape of the PDFs, only a translation of the mean. The need for piecewise detrending is demonstrated again in Figure 3g; however, this time we have a series which does exhibit a nonstationary variance, that is increasing with time. The PDFs (Figure 3h) show a large change in mean as well as becoming flatter and wider, indicating an increase in variance. Using the detrending method, we can see that the mean and variance have both increased (Figures 3i and 3j); however, the changes are not exaggerated as in Figures 3g and 3h.

[13] If we let $F_{Z^*_{s,k}}$ denote the Cumulative Probability Function (CDF), then the PDF can be denoted as $F'_{Z^*_{s,k}}$. $F'_{Z^*_{s,k}}$ was estimated using L-Moments which were calculated for each daily station time series in each of 9 independent periods (k) and a Generalized Extreme Value (GEV) distribution was fitted using the known relationship between L-Moments and the GEV [*Hosking*, 1990]. The GEV PDF $F'_{Z^*_{s,k}}$ given by equation (4) was chosen as it was consistently the best matched distribution (of six different distributions detailed in the work of *Hosking* [1990]) to DSMT (assessed using a Komolgorov-Smirnov test).

$$F'_{Z^*_{s,k}}\left(z^*_{s,k}(i)\right) = \frac{1}{\sigma_f}\left[1 + \xi_f\left(\frac{z^*_{s,k}(i) - \mu_f}{\sigma_f}\right)\right]^{-1/\xi_f - 1} \cdot \exp\left\{-\left[1 + \xi_f\left(\frac{z^*_{s,k}(i) - \mu_f}{\sigma_f}\right)\right]^{-1/\xi_f}\right\} \tag{4}$$

Where μ_f, σ_f, and ξ_f are the fitted (f) location, scale, and shape parameters of the GEV distribution, respectively.

[14] To visualize the regional mean PDF, we simply averaged each station's PDF within a region (equation (5)). R denotes one of four regions, i.e., the whole western European area (all 54 stations), Scandinavia (6 stations; 5 in Sweden and 1 in Finland), Iberian Peninsula (12 stations;

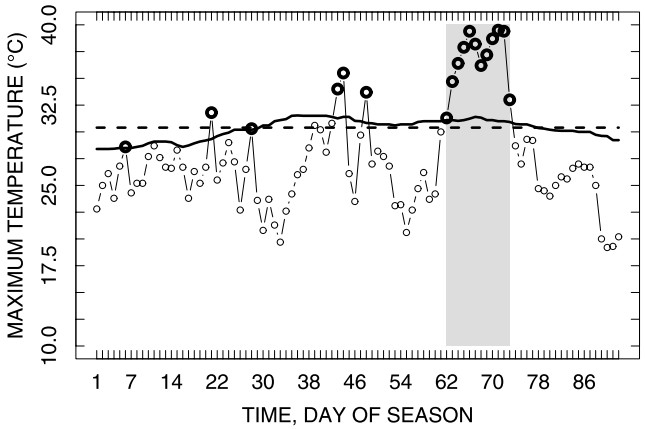

Figure 2. A time series of the DSMT 2003 measured in Paris. The thick black line (thick dashed black line) indicates the daily (seasonal) 95th percentile shown in Figure 1. Hot days (HD) are bold black open circles and the heat wave (HW) index has been calculated as the number of HDs in the period marked by a grey rectangle (12 days).

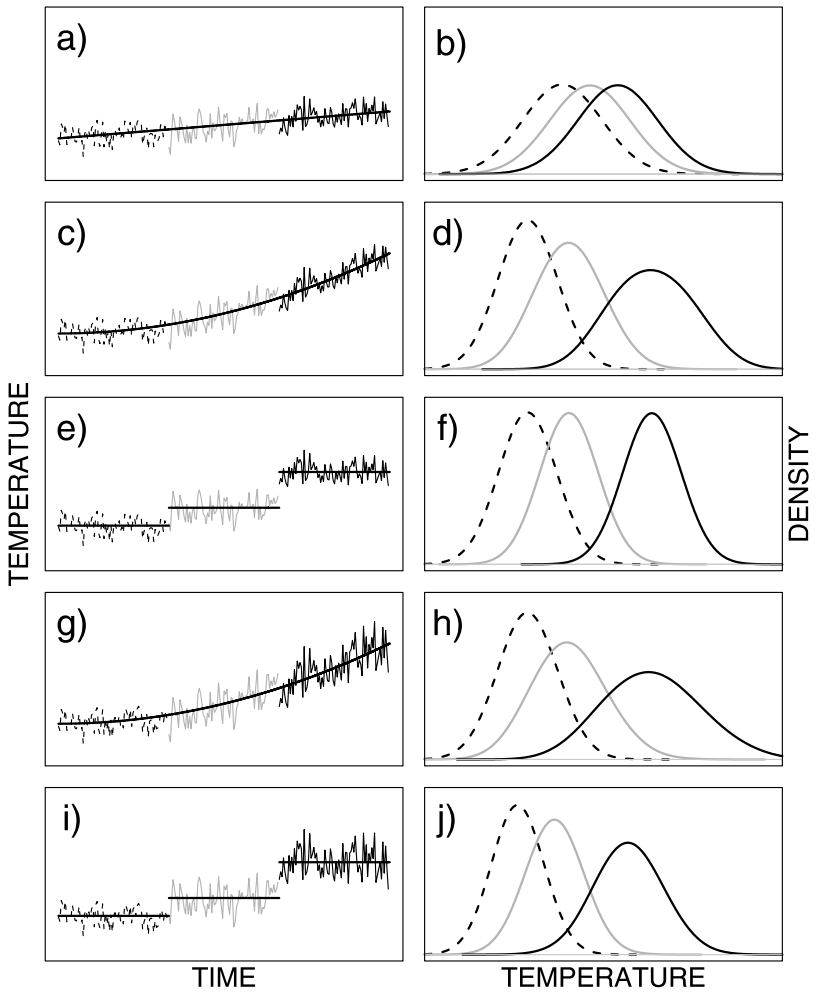

Figure 3. A conceptual diagram showing the piecewise detrending method (equation (3))] applied to the DSMT (adapted from *Scherrer et al.* [2005]). On the left are synthetic time series with (a) constant variance and a linear trend, (c) constant variance and a quadratic trend, (e) the quadratic series in Figure 3c after piecewise detrending, (g) a heteroscedastic series (increasing variance) with a quadratic trend, and (i) the heteroscedastic series in Figure 3g piecewise detrended. On the right, the corresponding PDF for each of the three independent periods in time series on the left is shown.

11 in Spain and 1 in Portugal), or central western Europe (36 stations; all remaining stations, not in the Scandinavia or Iberian Peninsula regions, see our recent work [*Della-Marta et al.*, 2007] for more details of each station series).

$$\bar{F}'_{Z^*_{s,k}}(R) = \frac{1}{n_s \in R} \sum_{s \in R=1}^{n_s \in R} F'_{Z^*_{s,k}} \tag{5}$$

[15] To show the interstation change in the mean, variance, and skewness of each station PDF (equation (5)) for each period k, we used the definitions of *Klein Tank et al.* [2005] which are given by the following equations, keeping the subscript s to denote the station number.

$$\mu_{s,k} = \bar{Z}_{s,k} = \frac{1}{N_{s,k}} \sum_{i=1}^{N_{s,k}} z_{s,k}(i) \tag{6}$$

$$\sigma_{s,k} = \frac{F_{Z^*_{s,k}}(0.9) - F_{Z^*_{s,k}}(0.1)}{2} \tag{7}$$

$$\gamma_{s,k} = \frac{F_{Z^*_{s,k}}(0.9) - F_{Z^*_{s,k}}(0.5)}{F_{Z^*_{s,k}}(0.5) - F_{Z^*_{s,k}}(0.1)} \tag{8}$$

Note that the units of equations (6), (7), and (8) are nondimensional. A value of 1.0 in equation (8) indicates that the PDF is not skewed, whereas values below 1.0 (above 1.0) indicate a negatively (positively) skewed PDF.

[16] To quantify the regional change in variance and skewness (equations (7) and (8)), a Robust Linear Model (RLM) was fitted according to equation (9) to the data points, $\sigma_{s,k}$.

$$\sigma_R(k) = \beta \sigma_{s \in R,k} + \epsilon_{s,k} \tag{9}$$

Where β is a vector of the RLM slope and intercept and ε is the vector of error terms in the regression and $k \in \{1, \ldots, 9\}$. Expressions for the percentage change in variance and skewness over the period 1880–2005 are given below.

$$\Delta\sigma_R = \frac{\sigma_R(9) - \sigma_R(1)}{9} \times 100.0 \quad (10)$$

Similarly, substituting $\gamma_{s\in R,k}$ into equation (9) for γ_R, we get:

$$\Delta\gamma_R = \frac{\gamma_R(9) - \gamma_R(1)}{9} \times 100.0 \quad (11)$$

[17] The change in mean temperature is quantified differently to the change in variance and skewness. We start by first calculating the regional daily average temperature anomaly (°C) using equation (12). Note that now, the abscissa in equation (12) is the daily time values and not independent periods k as in equation (9).

$$\bar{x}_R(i) = \frac{1}{n_{s\in R}} \sum_{s\in R=1}^{n_{s\in R}} (x_s(i) - \mu_s) \quad (12)$$

Then, an RLM was fitted to $\bar{x}_R(i)$,

$$\mu_R(i) = \beta\bar{x}_R(i) + \epsilon_i \quad (13)$$

with the corresponding change in temperature given by equation (14).

$$\Delta\mu_R = \frac{\mu_R(N) - \mu_R(1)}{N} \quad (14)$$

Where N = 11,592.

[18] Almost the same procedure (equations (2) to (14)) was used to assess the changes in the PDF of the extreme indices substituting HD and HW for Z. The extreme indices were not standardized (equation (1)) since both indices are percentile-based and therefore already consider the changes relative to the local climate of each station. Also, instead of fitting the GEV distribution (as in equation (4)), we fitted a Gamma distribution (using L-Moments), as it is zero-bounded and was found to provide a good fit to the index data. The extreme indices were split into 4 (not 9, as before) independent periods k (1880 to 1909, 1910 to 1939, 1940 to 1969, and 1970 to 2005). Since the indices are seasonally resolved, the independent period length k was chosen as a compromise between having detailed information on distribution changes over time and being able to calculate reliable L-Moment statistics [*Hosking*, 1990]. Sometimes the detrending of the independent periods k (equation (3)) resulted in negative HD and HW indices. We ignored these values since they can be considered part of the long-term variability we are trying to remove from the series in order to isolate the intrinsic variability.

3. Results and Discussion

3.1. Changes in the PDF of DSMT

[19] Both the mean and variance of DSMT averaged over western Europe have increased significantly since 1880. The PDF of western European DSMT has become flatter and wider (Figure 4a). This change becomes even more dramatic if we focus only on central western Europe (Figure 4b). In order to accurately assess the change in DSMT variance, data in each of the independent periods shown in Figures 4 and 5a and 5b has been detrended [*Scherrer et al.*, 2005], then the mean of that period has been added back to the data to show the change in mean and variance (equation (3)). Figure 5a shows that the standardized DSMT have increased by approximately 0.4 units (robust trend not shown), which corresponds to an equivalent rise in temperature of 1.6 ± 0.4°C from 1880 to 2005 (Figure 5c and Table 1). The increase in DSMT has not been monotonic [*Luterbacher et al.*, 2004; *Moberg et al.*, 2006]. The data show distinct decadal and multidecadal variability, as the 1936 to 1949 and the 1992 to 2005 period experienced anomalously higher average maximum temperatures (Figures 5a and 5c). Part of this variability has been attributed to the Atlantic Multidecadal Oscillation (AMO) [*Sutton and Hodson*, 2005], a long-term cycle in Atlantic Sea Surface Temperatures (SSTs) believed to be driven by the Atlantic Thermohaline Circulation (THC) [*Knight et al.*, 2005]. Other studies attribute the 1900∼1950 European temperature variability to natural forcings such as solar and volcanic influences [*Stott et al.*, 2004] and the relative cool period in the 1960s to the influence of sulfate aerosols [*Boer et al.*, 2000]. However, temperature increases in Europe over the last 50 years are mostly attributable to anthropogenic influence [*Stott et al.*, 2004; *Klein Tank et al.*, 2005].

[20] The variance of DSMT across western Europe has increased significantly by approximately 6 ± 2% and by 11 ± 2% for central western Europe (see Table 1). Figure 5b shows the general increase in DSMT variance, with the most distinct positive trend appearing from the 1950s. The results for this period agree with those of previous studies [*Klein Tank and Können*, 2003; *Klein Tank et al.*, 2005; *Scherrer et al.*, 2005]. However, they also highlight the need for longer, more robust data sets such as the one used here in order to place the recent temperature variability in the context of past variability [*IPCC*, 2001; *Luterbacher et al.*, 2004]. Interestingly, we see that the DSMT variance during the 1936 to 1949 period is high, a period with anomalously high temperatures (Figures 5a and 5c). This may indicate that the variance of DSMT is proportionally related to the mean DSMT. Interdecadal changes in the mean DSMT for central western Europe can account for approximately 14% of changes in DSMT variance as shown by Figure 6.

[21] Our observations of regional changes in mean and variance of DSMT fall in line with expected future summer temperatures. Central western Europe, the region with the largest observed increase in DSMT of 11 ± 2% (see Table 1 and Figure 5b) from 1880 onward, is also the region with the greatest expected change in summer temperature variability, with changes up to 100% by 2071 to 2100 [*Schär et al.*, 2004; *Weisheimer and Palmer*, 2005; *Seneviratne et al.*, 2006]. The expected large increase in temperature variability in central western Europe is believed to be driven in part by soil moisture, precipitation, and atmospheric circulation feedback processes [*Pal et al.*, 2004; *Schär et al.*, 2004; *Brabson et al.*, 2005; *Ferranti and Viterbo*, 2006; *Findell and Delworth*, 2005; *Seneviratne et al.*, 2006; *Fischer et al.*,

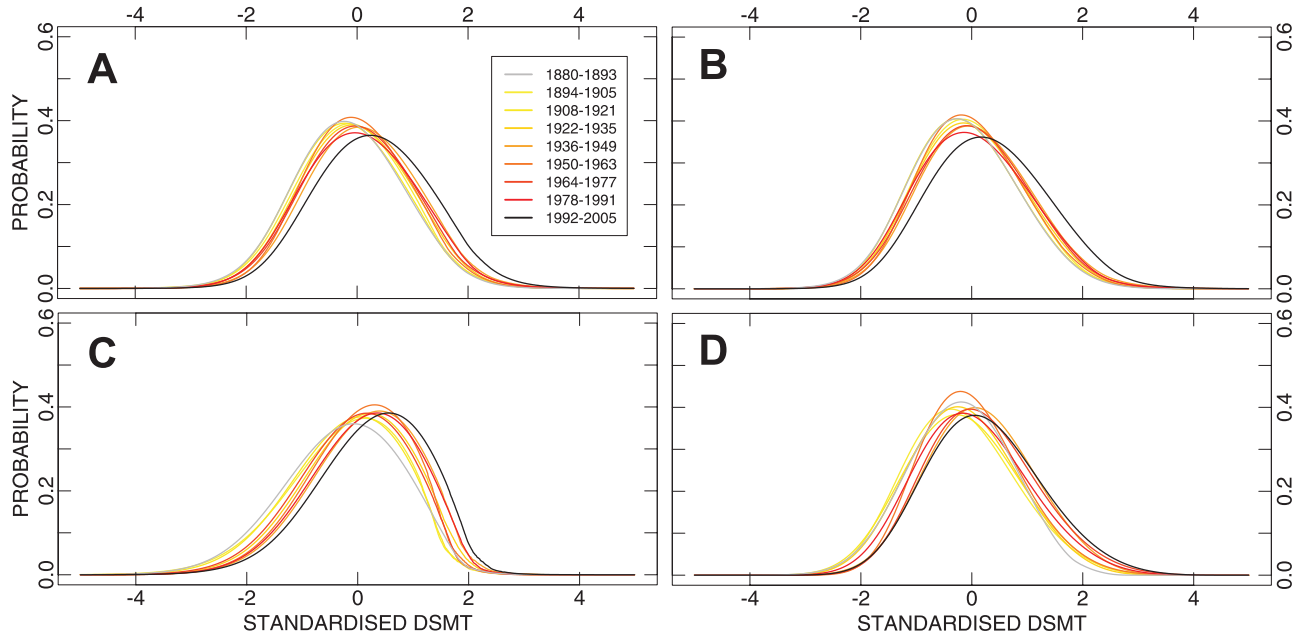

Figure 4. DSMT Probability Density Function (PDF) change over time for four different regions of western Europe. Each PDF is the average PDF of (a) 54 stations for each of nine independent periods for the entire western European domain, (b) 34 stations in central western Europe, (c) 12 stations in the Iberian Peninsula, and (d) 6 stations in Scandinavia. The colored PDFs represent the different independent periods according to the legend in the right of the Figure 4a. All DSMTs were standardized by the 1906 to 1990 mean and standard deviations and piecewise detrended, preserving the changes in mean DSMT for each independent period.

2007]. An anthropogenically induced warmer environment, together with expected and observed decreases in summer precipitation [*Ferranti and Viterbo*, 2006; *Findell and Delworth*, 2005; *Moberg et al.*, 2006; *Della-Marta et al.*, 2007], lead to a feedback threshold being exceeded with a dramatic increase (decrease) in sensible (latent) heat fluxes in the European summer climate [*Schär et al.*, 2004; *Ferranti and Viterbo*, 2006; *Seneviratne et al.*, 2006; *Fischer et al.*, 2007]. We have observed a significant negative trend in the observed DSMT variability over the Iberian Peninsula of $-7 \pm 3\%$ (Figure 4c, part of this negative trend may be due to remaining inhomogeneities [*Brunet et al.*, 2006]) and an increase of $4 \pm 6\%$ over Scandinavia (Figure 4d, also with a large increase in positive skewness). Likewise, according to regional climate model experiments [*Schär et al.*, 2004; *Seneviratne et al.*, 2006], the regions with the lowest change in variability expected by 2071 are southern western Europe, including the Iberian Peninsula, and northern western Europe, including Scandinavia, with changes in the order of 0 to 40%. As with variability, mean temperature change is observed (Table 1) and expected to be highest over southern Europe and the Iberian Peninsula, whereas mean temperature change is observed and expected to be lower over central western Europe [*Schär et al.*, 2004; *Seneviratne et al.*, 2006].

3.2. Sensitivity of Extremes on Changes in the DSMT PDF

[22] A consequence of increased DSMT mean and variance is an increase in the relative sensitivity [*Mearns et al.*, 1984; *Katz and Brown*, 1992; *Schär et al.*, 2004] of an extreme event exceeding a given threshold. According to the trends in western Europe, decadal PDF changes shown in Figure 4a and Table 1, the probability of a DSMT above the 90th, 95th, and 98th percentile has increased by approximately 193%, 233%, and 312%, respectively (relative to the 1906 to 1990 period, based on a robust linear trend, see section 2). If, for example, only the mean DSMT changed (as observed $+1.6 \pm 0.4^{\circ}$C) and was not accompanied by a variance increase (as observed $+6 \pm 2\%$), then the probability of a DSMT above the 90th, 95th, and 98th percentiles would only be 178%, 205%, and 252% greater. This is between 14 and 60% less than the probability change due to the combined mean and variance increase. If the variance of central western Europe DSMT did not increase by $11 \pm 2\%$, but only the mean changed ($+1.3 \pm 0.5^{\circ}$C), the difference in the frequency of extreme temperatures would be between approximately 22 and 84% less.

[23] Two extreme indices we call hot days (HD) and heat waves (HW) also demonstrate this sensitivity of extremes to changes in the mean and variance of DSMT. We find that almost all station records used in this analysis have a positive trend in the occurrence of summer HDs and HWs from 1880 to 2005 (Figures 7b and 7d). Around 80% of the trends are significant. The largest trends have been found over the Iberian Peninsula and in central western Europe. The time evolution of European average HDs (Figure 7a) shows an overall positive trend of $0.38 \pm 0.05\%$ of summer days per decade. This trend is equivalent to approximately a $188 \pm 54\%$ increase, with an average of 7.3% of summer

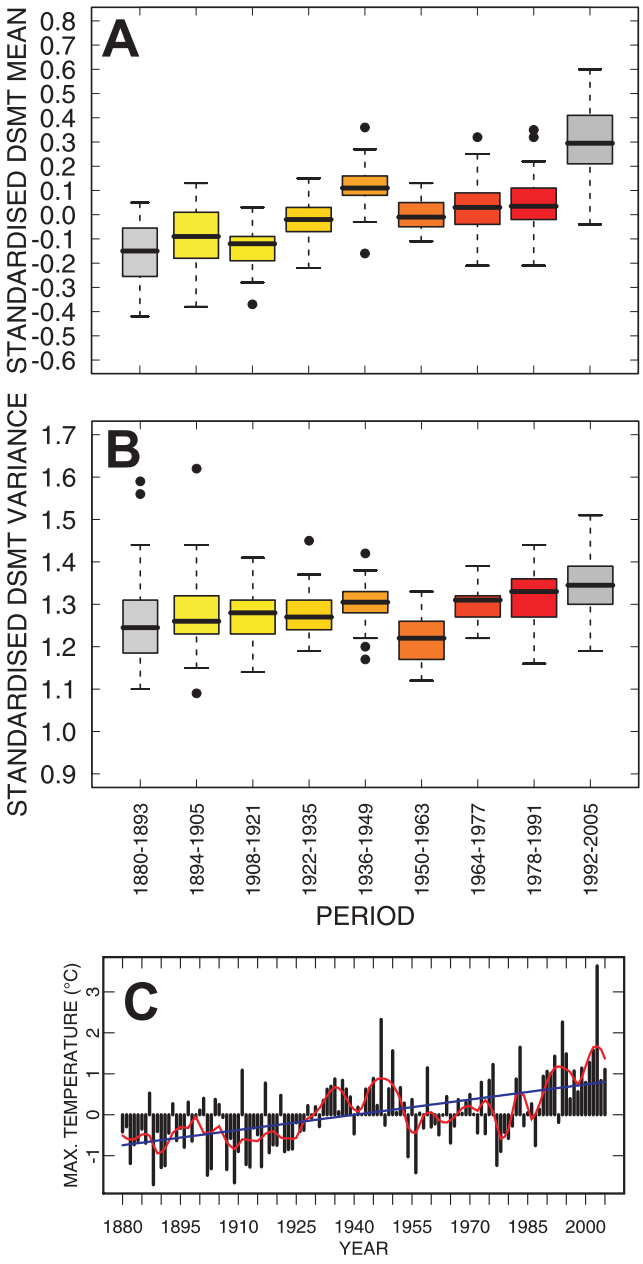

Figure 5. Interstation distribution of (a) western European standardized DSMT mean temperature for each independent period, (b) the standardized variance for each independent period, and (c) the interannual variability of western European temperature from 1880. The box plots in Figures 5a and 5b show the median (solid black line in the middle of the colored box), interquartile range (boundaries of the colored box), and 1.5 times the interquartile range (outer lines) and observations outside this range (black dots) of the standardized mean and variance, respectively. The black bars in Figure 5c are the average western European maximum temperature anomalies (with respect to the 1906 to 1990 mean), the blue line denotes the overall robust linear trend (Table 1), and the red curve denotes the decadal filtered series.

Table 1. DSMT Mean, Variance, and Skewness Trends From 1880 to 2005, for Each Region of Western Europe[a]

Region R (n_s)	$\Delta\mu_R$, °C	$\Delta\sigma_R$, %	$\Delta\gamma_R$, %
western Europe (54)	**+1.6 ± 0.4**	**+6 ± 2**	+0 ± 7
Central western Europe (36)	**+1.3 ± 0.5**	**+11 ± 2**	+0 ± 6
Iberian Peninsula (12)	**+2.6 ± 0.6**	−7 ± **3**	−1 ± 12
Scandinavia (6)	**+1.7 ± 0.7**	+4 ± 6	**+9 ± 6**

[a]Trends in variance and skewness have been calculated over nine independent periods. The mean, variance, and skewness trends are expressed in the units of °C, %, and % with respect to the 1906 to 1990 period, respectively. The error estimates are 95% confidence intervals based on the standard error of the robust linear fit. Figures quoted in boldface are significantly (5% significance) different from zero. The number of station time series n_s is shown in parentheses after each region name. See section 2 for more details on the calculations.

days classified as HDs at the end of the period, compared with 2.5% in 1880. The 6 ± 2% and the 11 ± 2% increase in DSMT variance over the whole of western Europe and central western Europe is responsible for approximately 25% and 40% of the increase in HDs in these regions, respectively. This confirms that small changes in the intrinsic variance of DSMT have lead to greatly amplified changes in the frequency of extremes. Similarly, the length of HWs has increased by approximately 111 ± 36%, from an average of 1.4 to 3.0 days per HW (Figure 7c). As a result, HWs have doubled in length over the period 1880 to 2005. The changes in the HW index are especially important since this index combines a measure of the extreme magnitude of the daily temperatures as well as a measure of their persistence. Prominent European extreme summer HW and HD seasons include 1911, 1947, 1976, 1994, and

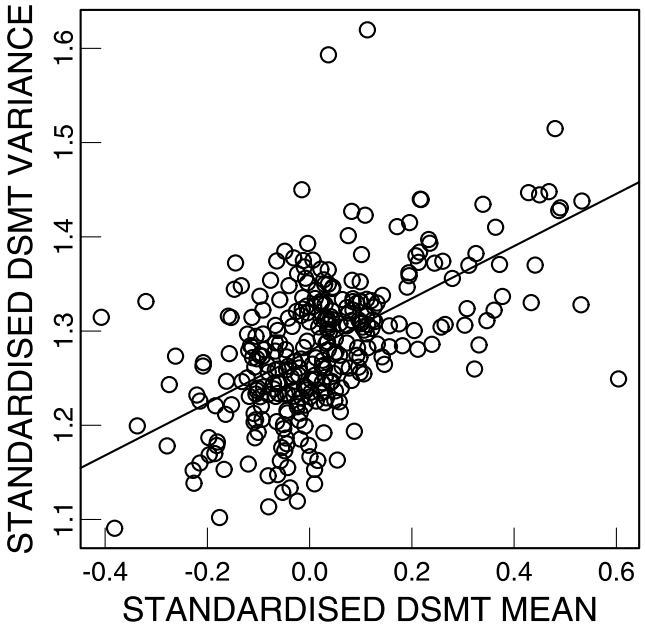

Figure 6. The relationship between DSMT standardized mean temperature and standardized variance for each of the nine independent periods for 36 stations in central western Europe 1880 to 2005. The linear trend has been fitted using Total Least Squares (TLS).

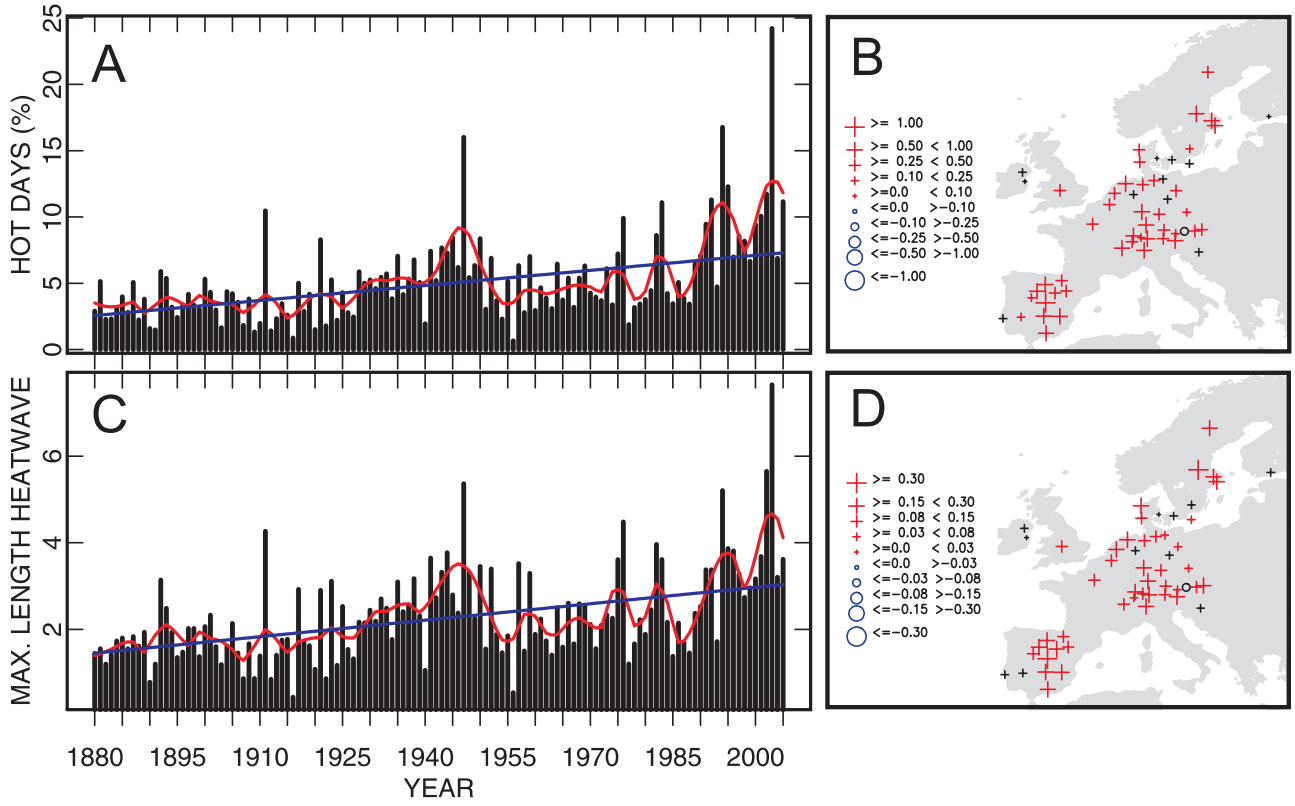

Figure 7. June-August (a) average number of western European hot days (HD) and (c) maximum length heat wave (HW) from 1880 to 2005. The long-term decadal variability (thick red line) and the overall robust linear trend (thick blue line) are shown. The units of HDs are percent of June-August days and the units of HWs are days. The spatial distribution of decadal (b) HD and (d) HW trends at each station. The sizes of the plus '+' and empty circles 'o' are proportional to the magnitude of the positive and negative trends, respectively, according to the legend left of the figure. Red- (black-) colored crosses indicate significant (nonsignificant) positive trends at the 5% significance level (similarly for negative trends).

2003 [*Klein Tank and Können*, 2003; *Schär et al.*, 2004; *Klein Tank et al.*, 2005; *Moberg et al.*, 2006; *Della-Marta et al.*, 2007; *Fischer et al.*, 2007]. Most of these events had regional differences in the extent and severity of the heat wave(s) not able to be shown here in these summary statistics. See the work of *Xoplaki et al.* [2003] and ours [*Della-Marta et al.*, 2007] for an overview of regional differences and large-scale influences on these and other events. *Fischer et al.* [2007] show a detailed analysis of the sensitivity of four extreme summers to soil moisture perturbations. They estimate that between 50 and 80% of the excess HDs can be explained by soil moisture deficits. Seasons in which there are a higher number of HDs correspond to seasons where the HW index is also higher, however, notice that the variability of the HD index is higher than the HW index (Figures 7a and 7c). The low-frequency, multidecadal component (Figures 7a and 7c, red line) shows a higher occurrence of HWs between 1880 to 1905, 1925 to 1950, and 1990 to 2003 periods relative to the linear fit (Figure 7c, blue line). Figure 8 shows the western Europe PDF of HDs and HWs for four separate periods. Both the HD and HW fitted distributions have become flatter and longer tailed from 1910. The probability of the maximum length HW in a particular season lasting 5

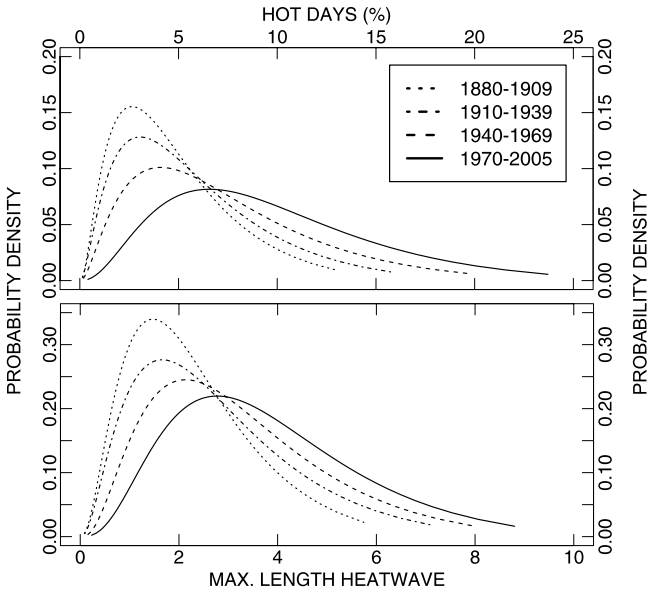

Figure 8. June-August PDF of (a) western European hot days (HD), and (b) maximum length heat wave (HW) for each of four independent periods according to the legend in the top right-hand corner of Figure 8a.

Table 2. A Summary of DSMT Mean and Variance and HD and HW Trends From 1880 to 2005 for Western Europe Using the Homogenized DSMT Data [*Della-Marta et al.*, 2007] and the Unhomogenized DSMT From *Moberg et al.* [2006][a]

Variable	Homogenized	Unhomogenized
$\Delta\mu_R$, °C	**+1.6 ± 0.4**	**+1.3 ± 0.2**
$\Delta\sigma_R$, %	**+6 ± 2**	**+5 ± 2**
ΔHD_R, %	**+188 ± 54**	**+125 ± 45**
ΔHW_R, %	**+111 ± 36**	**+79 ± 34**

[a]The error estimates are 95% confidence intervals based on the standard error of the robust linear fit. Figures quoted in boldface are significantly (5% significance) different from zero. See section 2 for more details on the calculations.

days or longer has increased from 0.03 to 0.14 over the last 126 years.

3.3. Effects of Daily Maximum Temperature Homogenization

[24] *Della-Marta et al.* [2007] homogenized 25 of the 54 station records used in this analysis using a new method that is explicitly designed to homogenize daily temperature measurements [*Della-Marta and Wanner*, 2006]. In Table 2, we show the differences in changes in DSMT PDF and HDs and HWs by using the additional 25 homogenized station records or by using the raw unhomogenized daily maximum temperature provided by the data providers listed in the work of *Moberg et al.* [2006]. Note that some of the station series in the work of *Moberg et al.* [2006] have been homogenized at the daily timescale by previous studies, see our recent work *Della-Marta et al.* [2007] and that of *Moberg et al.* [2006] for more details. Clearly, the use of these daily homogenized records has had an impact on the results presented in this paper. The effect is most obvious in the mean DSMT change with the estimate of change being an additional 0.3°C higher over the period 1880 to 2005. The method in our recent work [*Della-Marta and Wanner*, 2006] has been designed to remove inhomogeneities in the higher order moments of a PDF, such as variance and skewness; however, the impact of variance and skewness corrections seems to be low over the period 1880 to 2005 since the difference in the change in variance is only 1% higher using the new data set (Table 2). The homogenization has had a large impact on the estimates of the changes in the extreme indices HD and HW, with the percentage increase in HD and HW being 63% and 32% greater, respectively. The early instrumental temperature measurements in Europe, like most other measurements from around the world, are believed to be warm-biased due to the thermometers being exposed to greater extremes of sensible heat [*Parker*, 1994; *Nordli et al.*, 1997; *Moberg et al.*, 2003; *Della-Marta et al.*, 2007]. *Della-Marta et al.* [2007] also found that many of the 25 homogenized DSMT series tended to have inhomogeneously higher intrinsic variance in the late 19th and early 20th century than present, which is also likely to be a consequence of the poor instrument exposure. We believe that if more European daily temperature station series were corrected using a method such as that of our recent work [*Della-Marta and Wanner*, 2006], then the change in daily temperature variance measured over the last 126 years would be greater than quoted in this paper. A consequence of the lack of more homogenous daily temperature series in recent studies such as those of *Moberg et al.* [2006] and *Alexander et al.* [2006] is that their quoted long-term changes in summer extreme temperature indices in western Europe are likely to be conservative.

4. Conclusions

[25] For the first time, the intrinsic variability of western European DSMT has been analyzed with homogenized time series back to 1880. Western European DSMT intrinsic variance has increased significant since 1880. In agreement with previous studies [*Klein Tank et al.*, 2005], the most pronounced positive trend has been shown over the last 50 years. The combined changes in the mean and variance of DSMT PDF have contributed to an increase in the frequency of HDs and an increase in the persistence of HWs. Up to 40% of the changes in the frequency of HDs are attributable to an 11% increase in variance of the PDF.

[26] Matching with projections of temperature variance [*Schär et al.*, 2004; *Scherrer et al.*, 2005; *Weisheimer and Palmer*, 2005; *Seneviratne et al.*, 2006], the highest trends in DSMT variability have been found in central western Europe. The summer climate of this region has been found to be influenced by land-temperature and land-precipitation feedback processes which are critically dependant on soil moisture [*Schär et al.*, 2004; *Seneviratne et al.*, 2006; *Fischer et al.*, 2007]. Projected future warming in this region will enhance these feedback processes leading to a further increase in intrinsic temperature variability [*Schär et al.*, 2004; *Seneviratne et al.*, 2006]. Our observations could be used to support the theory that these processes have become dominant since around the 1950s. However, more studies, in addition to that of *Fischer et al.* [2007], should be performed in order to isolate the specific feedback processes and attribute cause and effect.

[27] We have shown new observational evidence that previous estimates of change in western European DSMT are likely to be conservative due to the warm biases in many late 18th and early 20th century temperature measurements. Previous estimates of DSMT change since 1880 are likely to be 0.3°C lower than previously thought.

[28] By the late 21st century, the persistence of long-lived heat waves lasting approximately 1.5 weeks in central western Europe is estimated to be around 50% longer than in the 1961 to 1990 period [*Meehl and Tebaldi*, 2004]. We show that over the last 126 years shorter lived but more intense heat waves have doubled in length. It remains a challenge for the meteorological community to understand more about these extreme events and for national health services to develop strategies to mitigate the effects of this increasing threat on human health [*Kovats and Koppe*, 2005].

Notation

- i counter to denote a daily maximum temperature measurement
- s counter to denote the station time series

X_s time series of daily maximum temperature at station s, °C
Z_s standardized time series of daily maximum temperature at station s
N_s number of daily maximum temperature observations
n_s number of station time series
μ_s long-term mean of daily maximum temperature at station s
σ_s long-term standard deviation of daily maximum temperature at station s
k counter to denote the independent period number
$Z_{s,k}$ standardized time series of daily maximum temperature at station s for period k
$N_{s,k}$ number of daily maximum temperature observations for station s in period k
$\rho(k)$ function that sets the starting point of the time series for period k
$\alpha_{s,k}$ intercept term of an ordinary least squares model for station s in period k
$\beta_{s,k}$ slope term of an ordinary least squares model for station s in period k
$z^*_{s,k}$ piecewise-detrended standardized time series at station s in period k
$\bar{Z}_{s,k}$ mean standardized time series at station s in period k
$F_{Z^*_{s,k}}$ Cumulative Probability Function (CDF) of the standardized time series at station s in period k
$F'_{Z^*_{s,k}}$ Probability Density Function (PDF) of the standardized time series at station s in period k
μ_f location parameter of the Generalized Extreme Value (GEV) distribution fitted using L-Moments
σ_f scale parameter of the Generalized Extreme Value (GEV) distribution fitted using L-Moments
ξ_f shape parameter of the Generalized Extreme Value (GEV) distribution fitted using L-Moments
R counter to denote a geographical region over which mean statistics for stations s within this region are calculated
$\bar{F}'^*_{Z_{s,k}(R)}$ regional R mean PDF of the piecewise detrended standardized time series at station s in period k
$\mu_{s,k}$ mean of standardized daily maximum temperature at station s in period k
$\sigma_{s,k}$ variance of standardized daily maximum temperature at station s in period k
$\gamma_{s,k}$ skewness of standardized daily maximum temperature at station s in period k
$\sigma_R(k)$ regional mean variance of the regional mean PDF for period k
$\gamma_R(k)$ regional mean skewness of the regional mean PDF for period k
β Robust Linear Model (RLM) regression coefficients, slope and intercept
ϵ error term in the RLM
$\Delta\sigma_R$ percentage change in the regional mean variance
$\Delta\gamma_R$ percentage change in the regional mean skewness
$\bar{x}_R$ regional R mean daily maximum temperature anomaly, °C
$\mu_R(i)$ regional daily mean maximum temperature
N length of the time series of fitted values from the RLM
$\Delta\mu_R$ change in the regional mean temperature, °C
ΔHD_R percentage change in the regional frequency of HD
ΔHW_R percentage change in the regional length of HW

[29] **Acknowledgments.** We wish to acknowledge Phil Jones, Thomas Stocker, Christoph Appenzeller, and Robert Glick for their comments on an earlier version of the manuscript. Three anonymous reviewers provided useful comments on our manuscript. P.D.M. and J.L. were financially supported through the European Environment and Sustainable Development program, project EMULATE, EVK2-CT-2002-00161. P.D.M. was also financially supported by the Swiss Science Foundation (NCCR Climate).

References

Alexander, L. V., et al. (2006), Global observed changes in daily climate extremes of temperature and precipitation, *J. Geophys. Res.*, *111*, D05109, doi:10.1029/2005JD006290.

Boer, G. J., G. Flato, M. C. Reader, and D. Ramsden (2000), A transient climate change simulation with greenhouse gas and aerosol forcing: Experimental design and comparison with the instrumental record for the twentieth century, *Clim. Dyn.*, *16*(6), 405–425.

Brabson, B. B., D. H. Lister, P. D. Jones, and J. P. Palutikof (2005), Soil moisture and predicted spells of extreme temperatures in Britain, *J. Geophys. Res.*, *110*, D05104, doi:10.1029/2004JD005156.

Brunet, M., O. Saladié, P. D. Jones, J. Sigró, E. Aguilar, A. Moberg, D. Lister, A. Walther, and López (2006), The development of a new dataset of Spanish daily adjusted temperature series (1850–2003), *Int. J. Climatol.*, *26*, 1777–1802.

Cassou, C., L. Terray, and A. S. Phillips (2005), Tropical Atlantic influence on European heat waves, *J. Clim.*, *18*, 2805–2811.

Christidis, N., P. A. Stott, S. Brown, G. C. Hegerl, and J. Caesar (2005), Detection of changes in temperature extremes during the second half of the 20th century, *Geophys. Res. Lett.*, *32*, L20716, doi:10.1029/2005GL023885.

De Groen, P. (1996), An introduction to total least squares, *Nieuw Arch. Wiskd., Vierde serie*, *14*, 237–253.

Della-Marta, P. M., and H. Wanner (2006), A method of homogenising the extremes and mean of daily temperature measurements, *J. Clim.*, *19*, 4179–4197.

Della-Marta, P. M., J. Luterbacher, H. von Weissenfluh, E. Xoplaki, M. Brunet, and H. Wanner (2007), Summer heat waves over western Europe 1880–2003, their relationship to large-scale forcings and predictability, *Clim. Dyn.*, *29*(2–3), 251–275, doi:10.1007/s00382-007-0233-1.

Ferranti, L., and P. Viterbo (2006), The European summer of 2003: Sensitivity to soil water initial conditions, *J. Clim.*, *19*, 3659–3680.

Findell, K. L., and T. L. Delworth (2005), A modeling study of dynamic and thermodynamic mechanisms for summer drying in response to global warming, *Geophys. Res. Lett.*, *32*, L16702, doi:10.1029/2005GL023414.

Fischer, E. M., S. I. Seneviratne, D. Luthi, and C. Schär (2007), Contribution of land-atmosphere coupling to recent European summer heat waves, *Geophys. Res. Lett.*, *34*, L06707, doi:10.1029/2006GL029068.

Hosking, J. R. M. (1990), *L*-Moments: Analysis and estimation of distributions using linear combinations of order statistics, *J. R. Stat. Soc.*, *52*, 105–124.

IPCC (2001), *Climate Change 2001: The Scientific Basis Contribution of Working Group I to the Third Assessment Report of the Intergovernmental Panel on Climate Change* (*IPCC*), Cambridge Univ. Press, New York.

Katz, R. W., and B. G. Brown (1992), Extreme events in a changing climate: Variability is more important than averages, *Clim. Change*, *21*, 289–302.

Kiktev, D., D. M. H. Sexton, L. Alexander, and C. K. Folland (2003), Comparison of modeled and observed trends in indices of daily climate extremes, *J. Clim.*, *16*, 3560–3571.

Klein Tank, A. M. G., and G. P. Können (2003), Trends in indices of daily temperature and precipitation extremes in Europe, 1946–99, *J. Clim.*, *16*, 3665–3680.

Klein Tank, A. M. G., G. P. Können, and F. M. Selten (2005), Signals of anthropogenic influence on European warming as seen in the trend patterns of daily temperature variance, *Int. J. Climatol.*, *25*, 1–16.

Knight, J. R., R. J. Allan, C. K. Folland, M. Vellinga, and M. E. Mann (2005), A signature of persistent natural thermohaline circulation cycles in observed climate, *Geophys. Res. Lett.*, *32*, L20708, doi:10.1029/2005GL024233.

Kovats, R.S., and C. Koppe (2005), Heatwaves past and future impacts on health, in *Integration of Public Health with Adaptation to Climate Change: Lessons learned and New Direction*s, edited by K. Ebi, J. Smith, and I. Burton, pp. 136–160, Taylor and Francis, Philadelphia, Pa.

Luterbacher, J., D. Dietrich, E. Xoplaki, M. Grosjean, and H. Wanner (2004), European seasonal and annual temperature variability, trends, and extremes since 1500, *Science*, *303*, 1499–1503.

Mearns, L. O., R. W. Katz, and S. H. Schneider (1984), Extreme high-temperature events: Changes in their probabilities with changes in mean temperature, *J. Clim. Appl. Meteorol.*, *23*, 1601–1613.

Meehl, G. A., and C. Tebaldi (2004), More intense, more frequent, and longer lasting heat waves in the 21st century, *Science*, *305*, 994–997.

Moberg, A., H. Alexandersson, H. Bergstroem, and P. D. Jones (2003), Were southern Swedish summer temperatures before 1860 as warm as measured?, *Int. J. Climatol.*, *23*, 1495–1521.

Moberg, A., et al. (2006), Indices for daily temperature and precipitation extremes in Europe analysed for the period 1901–2000, *J. Geophys. Res.*, *111*, D22106, doi:10.1029/2006JD007103.

Nordli, P. O., H. Alexandersson, P. Frich, E. J. Forland, R. Heino, T. Jonsson, H. Tuomenvirta, and O. E. Tveito (1997), The effect of radiation screens on Nordic time series of mean temperature, *Int. J. Climatol.*, *17*, 1667–1681.

Pal, J. S., F. Giorgi, and X. Q. Bi (2004), Consistency of recent European summer precipitation trends and extremes with future regional climate projections, *Geophys. Res. Lett.*, *31*, L13202, doi:10.1029/2004GL019836.

Parker, D. E. (1994), Effects of changing exposure of thermometers at land stations, *Int. J. Climatol.*, *14*, 1–31.

Poumadere, M., C. Mays, S. Le Mer, and R. Blong (2005), The 2003 heat wave in France: Dangerous climate change here and now, *Risk Anal.*, *25*, 1483–1494.

Schär, C., P. L. Vidale, D. Luthi, C. Frei, C. Haberli, M. A. Liniger, and C. Appenzeller (2004), The role of increasing temperature variability in European summer heat waves, *Nature*, *427*, 332–336.

Scherrer, S. C., C. Appenzeller, M. A. Liniger, and C. Schär (2005), European temperature distribution changes in observation and climate change scenarios, *Geophys. Res. Lett.*, *32*, L19705, doi:10.1029/2005GL024108.

Seneviratne, S. I., D. Lüthi, M. Litschi, and C. Schär (2006), Land-atmosphere coupling and climate change in Europe, *Nature*, *443*, 205–209.

Stott, P. A., D. A. Stone, and M. R. Allen (2004), Human contribution to the European heat wave of 2003, *Nature*, *432*, 610–614.

Sutton, R. T., and D. L. R. Hodson (2005), Atlantic Ocean forcing of North American and European summer climate, *Science*, *309*, 115–118.

Vautard, R., P. Yiou, F. D'Andrea, N. de Noblet, N. Viovy, C. Cassou, J. Polcher, P. Ciais, M. Kageyama, and Y. Fan (2007), Summertime European heat and drought waves induced by wintertime Mediterranean rainfall deficit, *Geophys. Res. Lett.*, *34*, L07711, doi:10.1029/2006GL028001.

Venables, W. N., and B. D. Riply (2002), *Modern Applied Statistics with S*, Springer, New York.

Weisheimer, A., and T. N. Palmer (2005), Changing frequency of occurrence of extreme seasonal temperatures under global warming, *Geophys. Res. Lett.*, *32*, L20721, doi:10.1029/2005GL023365.

Xoplaki, E., J. Gonzalez-Rouco, J. Luterbacher, and H. Wanner (2003), Mediterranean summer air temperature variability and its connection to the large-scale atmospheric circulation and SSTs, *Clim. Dyn.*, *20*, 723–739.

P. M. Della-Marta, Climate Services, Federal Office for Meteorology and Climatology, MeteoSwiss, Krähbühlstrasse 58, Zurich, CH-8044, Switzerland. (paul.della-marta@meteoswiss.ch)

M. R. Haylock, Climatic Research Unit, University of East Anglia, Norwich, UK.

J. Luterbacher and H. Wanner, Institute of Geography, University of Bern, Bern, Switzerland.